CHALMERS
UNIVERSITY OF TECHNOLOGY

Quantify and mimic the feedback through the steering wheel during specific driving conditions

Reproducing the steering feel in a conventional steering system in a Steer-by-Wire system

Master's thesis in Mobility engineering, MSc

Aron Dalemo

Department of Mechanics and Maritime Sciences
CHALMERS UNIVERSITY OF TECHNOLOGY
Gothenburg, Sweden 2023
www.chalmers.se

Master's thesis 2023

Quantify and mimic the feedback through the steering wheel during specific driving conditions

Reproducing the steering feel in a conventional steering system in a Steer-by-Wire system

ARON DALEMO

CHALMERS
UNIVERSITY OF TECHNOLOGY

Department of Mechanics and Maritime Sciences
Division of Vehicle Engineering and Autonomous Systems
Chalmers University of Technology
Gothenburg, Sweden 2023

Quantify and mimic the feedback through the steering wheel during specific driving conditions
Reproducing the steering feel in a conventional steering system in a Steer-by-Wire system
ARON DALEMO

Supervisor: Marcus Sjöberg, Manager of Vehicle Dynamics & Special Projects, Polestar
Examiner: Mats Jonasson, Senior researcher at the Division of Vehicle Engineering and Autonomous Systems, Chalmers

Master's Thesis 2023
Department of Mechanics and Maritime Sciences
Division of Vehicle Engineering and Autonomous Systems
Chalmers University of Technology
SE-412 96 Gothenburg
Telephone +46 31 772 1000

Cover: Interior of a Polestar 2

Typeset in LaTeX
Printed by Chalmers Reproservice
Gothenburg, Sweden 2023

Quantify and mimic the feedback felt through the steering wheel at specific driving conditions
Reproducing the steering feel in a conventional steering system in a Steer-by-Wire system
ARON DALEMO
Department of Mechanics and Maritime Sciences
Chalmers University of Technology

Abstract

The mobility industry is going through a transformation where mechanical-connected steering system is replaced with wired-connected steering system, called Steer-by-Wire. Steer-by-Wire steering feedback is set by a Electronic Control Unit.

Based on this transformation Polestar's dynamic department wants to create steering feedback in the coming Steer-by-Wire cars that mimic the feedback felt in a mechanical steering system during some specific conditions. This thesis aim is therefore to create software that creates feedback that mimics the mechanical system during these conditions:

- Driving over crest while turning
- Driving on a dashed road marking
- Driving across rutted roads
- Driving with front or rear axle saturated

The method starts with logging the sensors data from the car which should be converted to Steer-by-Wire when it is driving through the specific conditions to see how they could be detected. Then a car with a mechanically connected system is driven through the same conditions to see what the desired feedback should be.

The result is a Simulink model consisting of several functions, a main feedback function that sets the basic feedback and additional functions that are connected to the specific conditions.

The main feedback function has promising results. The functions that detect driving over crest while turning, dashed road marking and axle saturation show potential. These functions detect the situations and output the aimed feedback. For rutted road conditions, no solution for a function has been found.

In addition to the functions detecting the situation there are two functions for friction coefficient estimation to enable change of feedback in the steering wheel with available friction. These functions only show reasonable values when close to limit handling or steady state.

Keywords: Steer-by-wire, Steering feedback

Acknowledgements

First I would like to thank Polestar for the thesis opportunity. Your support has been fantastic. The list of employees that have helped me is long but just to mention a few: Mats Olsson and Alexander Sjögren who has helped me with setting up the test cars and logging data from them. Anton Albinsson has helped me with his knowledge in Simulink and vehicle dynamic models. Anders Larsson and Fredrik Lundqvist who has helped me with the on-limit test driving as well as opinions on how the steering should feel. Anders has also always taken his time to discuss this subject. A special thanks to my supervisor Marcus Sjöberg for always providing the resources and opportunities needed to make this work happen.

I also must mention Volvo Cars and their employees who have taken their time to support in supplying measuring equipment to the test vehicles.

Dana Köhn and Vector have been fanstastic with the support with software and hardware to measure data from the cars.

Last but not least I would like to thank for the support from Chalmers and especially my examiner Mats Jonasson who has helped me in this thesis.

Aron Dalemo, Gothenburg, May 2023

List of acronyms

Below is the list of acronyms that have been used:

CAN	Controller Area Network
ECU	Electronic Control Unit
EPAS	Electric Powered Assisted Steering
FBD	Free Body Diagram
FFT	Fast Fourier Transform
GPS	Global Positioning System
HPAS	Hydraulic Power Assisted Steering
HS	Height Sensors
SbW	Steer-by-Wire

Nomenclature

The parameters and variables used:

Parameters

l_i	$[m]$	Distance from front/ rear axle to neutral point in car
w_i	$[m]$	Track width front/ rear axle
L	$[m]$	Wheel base
g	$[m/s^2]$	Gravity of Earth
t_m	$[m]$	Mechanical trail
t_r	$[m]$	Trail from steering rack to kingpin axis
I_i	$[kgm^2]$	Inertia
m_i	$[kg]$	Mass

Variables

t_{pfi}	$[m]$	Pneumatic trail
$\delta_{f,i}$	$[rad]$	Steering angle front
ω_z	$[rad/s]$	Yaw Rate
β_{ij}	$[rad]$	Body slip angle
α_{ij}	$[rad]$	Side slip angle
v_i	$[m/s]$	Velocities
a_i	$[m/s^2]$	Accelerations
F_{kij}	$[N]$	Force
θ_p	$[rad]$	Pinion angle
θ_{SW}	$[rad]$	Steering wheel angle
θ_{FM}	$[rad]$	Feedback motor angle
θ_{tb}	$[rad]$	Torsion bar angle

Contents

List of Figures

List of Tables

1
Introduction

The mobility industry is going through a transformation where mechanical connections are replaced with software connections. One of those is the connection between the steering wheel and the wheels. The axle is replaced with two motors, creating a Steer-by-Wire system, referred to as SbW [1]. When replacing the axle the steering feedback that went through it must be implemented in the motor with an Electronic Control Unit, referred to as an ECU [2].

Polestar is working on implementing a SbW with the goal of mimicking the steering feedback of a connected steering system.

1.1 Aim

Mimicking a connected steering systems feedback in a Steer-by-Wire during the specific driving conditions:

- Driving over crest while turning.
- Driving on a dashed road marking.
- Driving across rutted roads.
- Driving with front or rear axle saturated.

1.2 Limitations

The limitation is set due to the available time and resources for the project.

- Only two vehicle is used for data measuring.
- No steering robot has been used.
- The reference vehicle is a hydraulic-assisted vehicle.
- For each specific condition a limited set of maneuvers is used.
- The resulting functions are not implemented in a SbW car.
- No state and disturbance estimator is included.

1.3 Specification of the issue under investigation

For the specific conditions, the following questions are asked:

- How can a function detect the specific conditions with the available signals?
- What is the feedback torque in the steering wheel for the connected steering system?

- How can the output of the function be set up to mimic feedback in a connected steering system? Can additional torque be added to enhance the feedback?

1.4 Ethical, ecological and social impact of thesis

A positive ethical aspect for developing SbW could be safety, because the steering system component can be packaged better, compared to the electrical and hydraulic-assisted steering system, which makes the risk of personal injuries in an accident less likely. A negative ethical perspective for the SbW is that the risk of loss in steering could be argued to be higher.

From an ecological perspective developing a SbW could lead to more driving because the comfort of the car could be increased. Increased driving is negative because it generally leads to increased pollution of nature. From a social perspective, increased driving could be positive if it leads to a more efficient and social society.

2
Theory

2.1 Steering feedback

The definition of steering feedback, sometimes referred to as steering feel, can be defined as the torque from the steering wheel to the driver seen in Figure 2.1 [3].

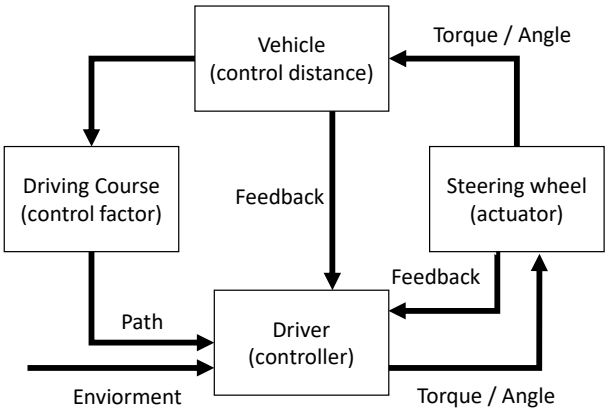

Figure 2.1: A schematic feedback illustration.

2.1.1 Ideal steering feedback

Ideal steering feedback is the feedback that informs the driver about the current situation. This could include disturbances, to make the driver have a haptic connection to the road [3][4].

Ideal feedback has an indiscernible delay in the dynamic behavior. The self-aligning torque in the steering wheel is precise and increases with lateral accelerations and has an automatic steering return. The center position of the steering wheel is distinct [2][3].

2.2 Steering-system configuration

This section covers the three assisted steering system configurations used in new cars, Hydraulic-Powered-Assisted, Electric-Powered-Assisted and Steer-by-Wire steering systems.

2.2.1 Hydraulic-Powered Assisted Steering

The assisting force in Hydraulic-Powered Assisted Steering, here called HPAS, comes from a pump pressuring fluid from a tank. A schematic picture of the system can be seen in Figure 2.2.

The pressurized fluid flows through a value which controls its path. The fluid flows back through the value to the pump until a steering torque from the drive is applied. Then the value redirects some of the flow to the rack, where a hydraulic piston transforms the pressurized fluid to a longitudinal force. The opening of value is mechanically controlled and depends on the torque applied, making the assisted force proportional to the torque from the driver [3].

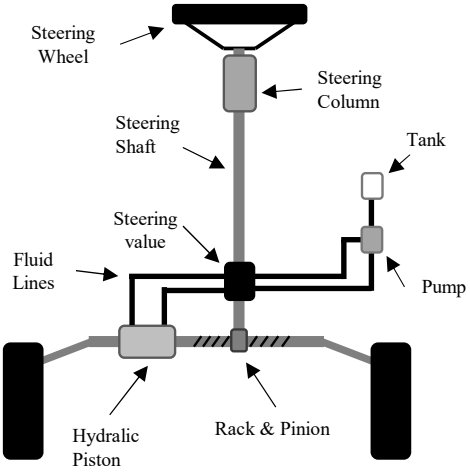

Figure 2.2: Schematic layout of a HPAS.

2.2.2 Electric-Powered Assisted Steering

Electric-Powered Assisted Steering, here referred to as EPAS, is a steering system where the driver is assisted by an electric motor. A schematic picture of this can be seen in Figure 2.3.

The motor is powered by the car's electric system and controlled with an integrated ECU, that transforms the input from the torque sensor located at the steering shaft to torque output to the motor. The advantage of the EPAS is lower power consumption plus added functionality compared to HPAS. The drawback is the added inertia where feedback can get filtered out before reaching the driver [3].

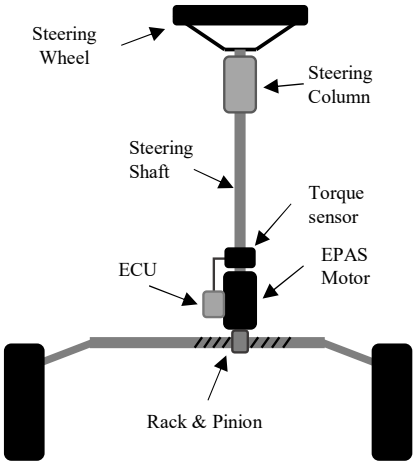

Figure 2.3: Schematic layout of a EPAS.

2.2.3 Steer-by-Wire

For a SbW, the steering wheel and the pinion are connected to two separate motors that are controlled by an ECU connected to sensors. A schematic diagram of the system can be seen in Figure 2.4.

The advantage of the SbW compared to the HPAS and EPAS is the packaging and safety aspect. The motor placements are more flexible and therefore easier to package safely. Another advantage is the extra degree of freedom for the disconnected steering wheel which gives completely customized feedback and added function possibilities. The drawback of SbW compared to the other two is a higher cost, weight, and complexity [3].

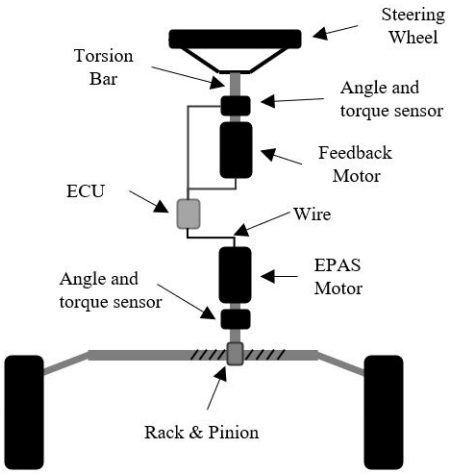

Figure 2.4: Schematic layout of a SbW.

2.3 Controlling of SbW system

The control of the feedback motor is either an open- or closed-loop with either angle or torque feedback. Closed-loop using torque control has better tracking performance and is more robust compared to the other options [5]. An example of the SbW closed loop system using torque control can be seen in Figure 2.5 where *Disturbance Estimator* removes measurement noise, *Feedback Calculation Function* decides the feedback and *controller* implement the feedback [3][5][6].

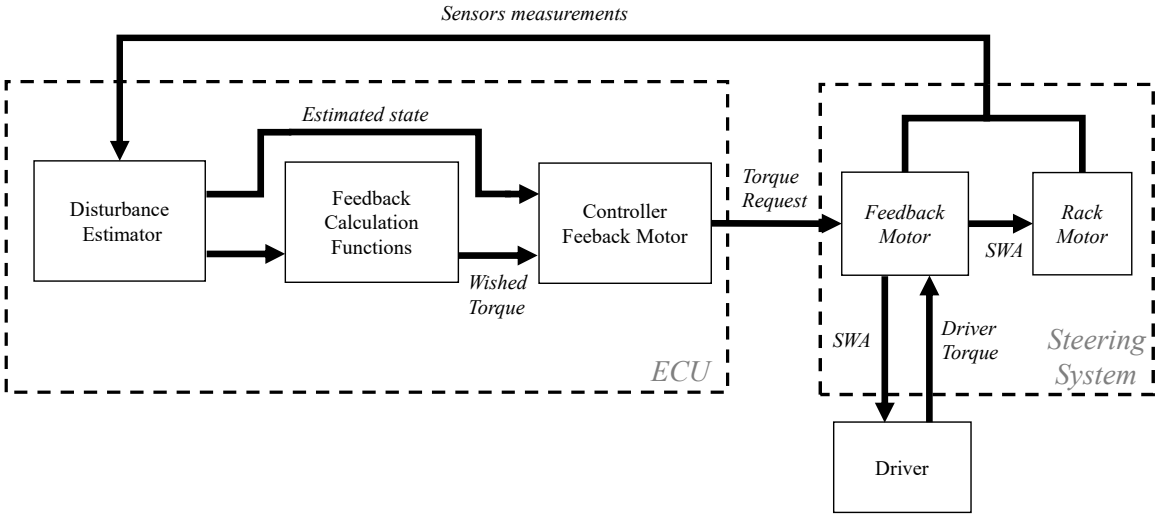

Figure 2.5: SbW control overview.

To calculate the torque in the steering wheel based on the torque in the *Feedback Motor*, a transfer function from a FBD, Free Body Diagram, can be set up, shown in Figure 2.6.

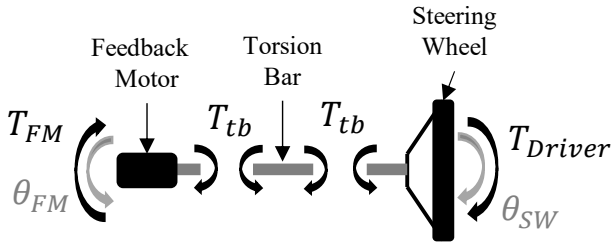

Figure 2.6: FBD of the steering wheel and feedback motor.

Where T_{FM} and θ_{FM} is the torque and angle for the feedback motor. While T_{Driver} and θ_{Driver} is the torque and angle from the driver and T_{TB} is the torque in the torsion bar. From the FBD can three equations from Newton's second law be set up, assuming to have viscous friction present.

$$I_{SW} \cdot \ddot{\theta}_{SW} = T_{Driver} - B_{SW} \cdot \dot{\theta}_{SW} - T_{TB} \tag{2.1}$$

$$T_{TB} = K_{TB} \cdot (\theta_{SW} - \theta_{FM}) + B_{TB} \cdot (\dot{\theta}_{SW} - \dot{\theta}_{FM}) \tag{2.2}$$

$$\ddot{\theta}_{FM} \cdot I_{FM} = T_{TB} - T_{FM} - B_{FM}\dot{\theta}_{FM} \tag{2.3}$$

Inserting equation 2.2 into equation 2.1 and 2.3 gives the following equations:

$$I_{SW} \cdot \ddot{\theta}_{SW} = T_{Driver} - B_{SW} \cdot \dot{\theta}_{SW} - K_{TB} \cdot (\theta_{SW} + \theta_{FM}) - B_{TB} \cdot (\dot{\theta}_{SW} + \dot{\theta}_{FM}) \tag{2.4}$$

$$I_{FM} \cdot \ddot{\theta}_{FM} = K_{TB} * (\theta_{SW} - \theta_{FM}) + B_{TB} \cdot (\dot{\theta}_{SW} - \dot{\theta}_{FM}) - T_{FM} - B_{FM}\dot{\theta}_{FM} \tag{2.5}$$

Then can a linear state space be created on the form:

$$\dot{x} = A \cdot x + B \cdot u \quad y = C \cdot x \tag{2.6}$$

The input to the system is the driver- and motor torque. The resulting output is the torque in the torsion bar, the angles of the steering wheel and motor. The state-, input- and output matrixes become:

$$x = \begin{bmatrix} \theta_{SW} \\ \dot{\theta}_{SW} \\ \theta_{FM} \\ \dot{\theta}_{FM} \end{bmatrix} \quad y = \begin{bmatrix} T_{tb} \\ \theta_{SW} \\ \theta_{FM} \end{bmatrix} \quad u = \begin{bmatrix} T_{Driver} \\ T_{FM} \end{bmatrix} \tag{2.7}$$

The matrices based on equations 2.4-2.5 and states-, output- and input-matrices from 2.7 are:

$$A = \begin{bmatrix} 0 & 1 & 0 & 0 \\ \frac{-K_{TB}}{I_{SW}} & \frac{-B_{TB}-B_{SW}}{I_{SW}} & \frac{K_{TB}}{I_{SW}} & \frac{B_{TB}}{I_{SW}} \\ 0 & 0 & 0 & 1 \\ \frac{K_{TB}}{I_{FM}} & \frac{B_{TB}}{I_{FM}} & \frac{-K_{TB}}{I_{FM}} & \frac{-B_{TB}-B_{SW}}{I_{FM}} \end{bmatrix} \quad B = \begin{bmatrix} 0 & 0 \\ \frac{1}{I_{SW}} & 0 \\ 0 & 0 \\ 0 & \frac{-1}{I_{SW}} \end{bmatrix}$$

$$C = \begin{bmatrix} K_{TB} & B_{TB} & -K_{TB} & -B_{TB} \\ 1 & 0 & 0 & 0 \\ 0 & 0 & 1 & 1 \end{bmatrix}$$

That is the state space that covers the steering wheel assembly in Figure 2.6 [2][5].

2.3.1 Main feedback function

The *Feedback Calculation Function* block, presented in Figure 2.5, can be built up as seen in Figure 2.7 which is based on [5]. Each block is explained in more detail.

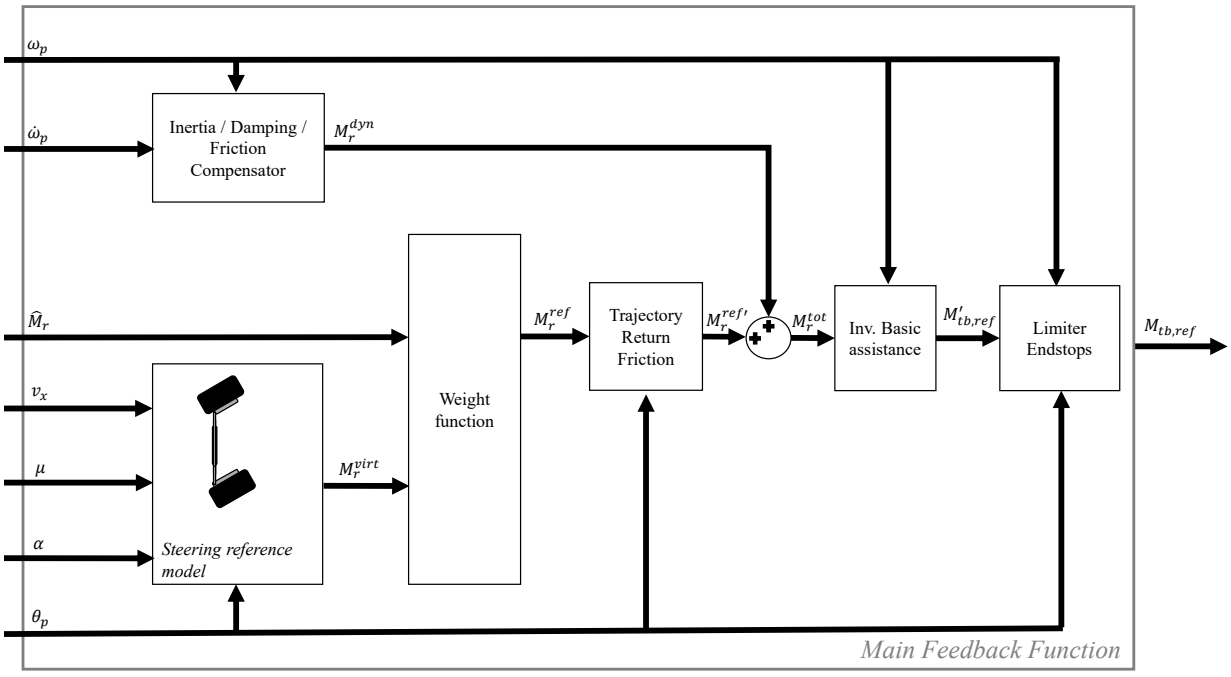

Figure 2.7: Feedback calculation block.

Where θ_p, ω_p and $\dot{\omega}_p$ is the steering pinion angle, angular speed and acceleration. Furthermore is $\hat{M}_r$ the measured steering torque, from the motor in the steering rack.

Inertia / Damping / Friction compensation
Calculates a torque to compensate for the inertia, damping, and Coulomb friction in the rack with the following equation

$$M_r^{dyn} = I_r \cdot \dot{\omega}_p(t) + b_r \cdot \omega_p(t) + M_{c-fricct} \tag{2.8}$$

Where I_r and b_r are linearized solutions from measurements at different velocities. The moment contribution from friction, $M_{c-fricct}$ is dependent on velocity and is estimated using a steady state maneuver [5].

Steering reference model

Based on longitudinal velocity (v_x), steering angle (θ_p), estimated friction (μ), slip angle (α), and a model of a steering system, the ideal feedback torque is calculated [5].

Weight function
To get feedback from both the ideal situation and the measured, this block mixes these torques [5].

Trajectory return friction
Adds damping to the steering equilibrium return motion, to ensure stability. It is done by changing the reference stiffness with the nonlinear equation:

$$\delta(t) = 1 + (\delta_0 - 1)(1 - e^{-r \cdot \theta_p^2 \cdot \omega_p^2}) \tag{2.9}$$

Where r is the dissipation rate and δ_0 is a reduction factor. Then is $\delta(t)$ added to the steering torque by the following condition:

if $\theta_p \cdot \omega_p < 0$
$\quad M_r^{ref'}(t) = \delta_0 \cdot M_r^{ref}(t)$
else
$\quad M_r^{ref'}(t) = M_r^{ref}(t)$
end

Where $M_r^{ref'}(t)$ is the output [5].

Inv. Basic assistance
This function decides based on the estimated torque how much torque the driver should feel. The correlation can be represented with the non-linear factor K_{assist} in the following equation [5]:

$$M'_{tb,ref} = K_{assist}(v_x, M_r^{tot}) \cdot M_r^{tot} \tag{2.10}$$

Limiter endstops
This function creates a virtual steering limit before the mechanical limits are reached. When θ_p is getting close to its limit an additional counteracting torque is added. The dependency is set up as:

$$M_{end}(t) = c_1(|\theta_p| - \theta_{end}) + k_1 \cdot |\omega_p(t)| \tag{2.11}$$

Where c_1 and k_1 are the end stop damping and stiffen parameters [5].

2.4 Reference model

The reference model estimate unknown variables with known variables and a virtual version of the vehicle. This project uses a four-track reference model [7], seen in Figure 2.8:

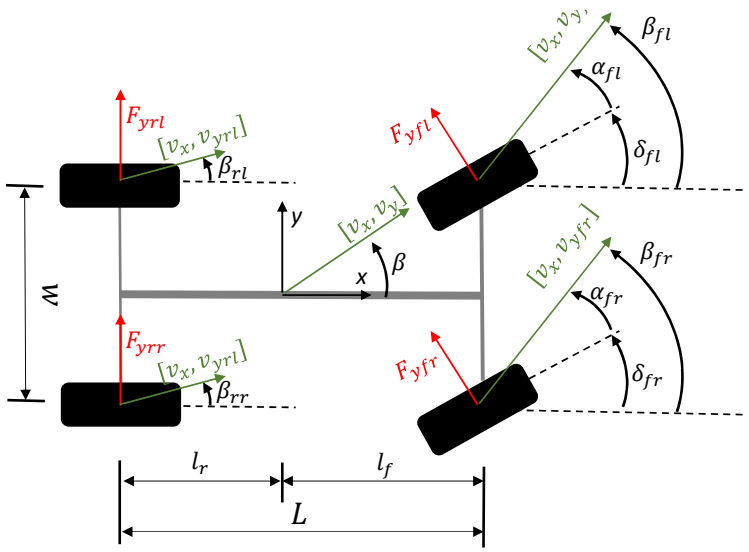

Figure 2.8: Simplified car geometry.

Based on Newton's second law can the following equation be set up

$$I_z \cdot \dot{\omega}_z = (F_{yfl} \cdot cos(\delta_{yfl}) + F_{yfr} \cdot cos(\delta_{yfr})) \cdot l_f - (F_{yrl} + F_{yrr}) \cdot l_r \tag{2.12}$$

$$a_y = -v_x \cdot \omega_z + \frac{F_y}{m} \tag{2.13}$$

A detailed description of how the unknown variables in the equation above are estimated is described in the coming sections.

2.4.1 Tire estimation

This section presents how the forces and velocities angles for the tires are estimated.

2.4.1.1 Slip estimation

To use the FBD in Figure 2.8 the slip angles, α_{fi} and β_{ri}, is estimated with the following equations:

$$\begin{aligned}
\alpha_{fl} &= \delta_{f,l} - atan\left(\frac{v_y(t) + l_f \cdot \omega_z(t)}{v_x(t) - 0.5 \cdot w_f \cdot \omega_z(t)}\right) \\
\alpha_{fr} &= \delta_{f,r} - atan\left(\frac{v_y(t) + l_f \cdot \omega_z(t)}{v_x(t) + 0.5 \cdot w_f \cdot \omega_z(t)}\right) \\
\beta_{rl} &= -atan\left(\frac{v_y(t) - l_r \cdot \omega_z(t)}{v_x(t) - 0.5 \cdot w_r \cdot \omega_z(t)}\right) \\
\beta_{rr} &= -atan\left(\frac{v_y(t) - l_r \cdot \omega_z(t)}{v_x(t) + 0.5 \cdot w_r \cdot \omega_z(t)}\right)
\end{aligned} \tag{2.14}$$

Where w_f and w_r are the track width, l_f and l_r are the distance to the neutral point. The lateral velocity is either measured or integrated from lateral acceleration, which is measured or estimated by Newton's second law. With Newton's second law, the

lateral forces are used and they are dependent on the slip which is dependent on lateral velocity, leading to an optimization problem [5][7].

The camber slip and turning slip can also be included. These are having less influence on the slip than the side slip [8].

2.4.1.2 Tire force estimation

The forces acting between the tire and the road can be estimated, both the size and the location, in several ways. This project uses curve-fit models. Where the model is tuned with parameters to fit measured data [7].

2.4.1.2.1 TMSimple is a curve-fit tire model based on the following equation [9][10][11][12]:

$$F_i(\alpha) = F_{max} \cdot sin(B \cdot (1 - e^{-|\alpha|/A}) \cdot sign(\alpha) \tag{2.15}$$

Where

$$B = \pi - arcsin(F_s/F_{max}) \tag{2.16}$$

$$A = F_{max} \cdot B/C \tag{2.17}$$

Where F_{max}, F_s and C are defined as seen in Figure 2.9.

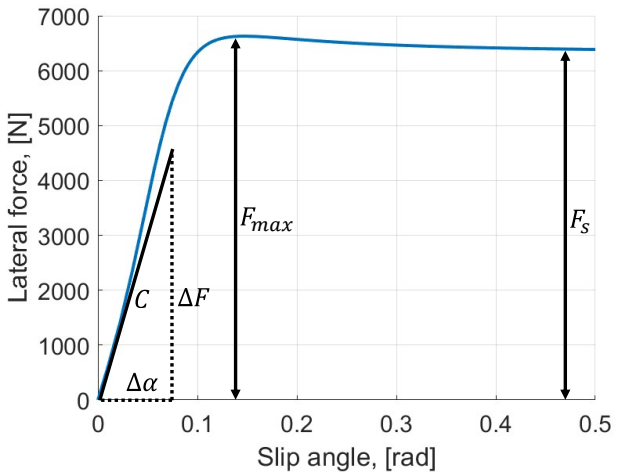

Figure 2.9: Definition of TMSimple variables.

2.4.1.2.2 Magic tire formula is a curve fit tire estimation purposed by Pacejka. It uses the following equation:

$$F_{yfi} = D_{yfi} \cdot sin(C_{yfi} \cdot atan(B_{yfi} \cdot \alpha_i) - E_{yfi}(B_{yfi} \cdot \alpha_i - atan(B_{yfi} \cdot \alpha_i))) \tag{2.18}$$

Where the slip stiffens, B_{yfi}, is defined by:

$$B_{yfi} = \frac{K_{y\alpha_i}}{C_{yi} \cdot D_{yi}} \tag{2.19}$$

Where $K_{y\alpha_i}$ is defined as

$$K_{y\alpha_i} = C_{\alpha_i 0} \cdot sin(2 \cdot atan(F_{zi}/(p_{Kyi} \cdot F_{z,nom})))\lambda_{Kyi} \tag{2.20}$$

And the maximum lateral tire potential, D_{yfi}, is defined as:

$$D_{yfi} = \sqrt{(\lambda_{\mu yi} \cdot \mu_{y_0} \cdot F_{zi})^2 - F_{xi}^2} \tag{2.21}$$

Furthermore, C_{yi} is the shape factor, C_α is the tire cornering stiffness and p_{Kyi} λ_{Kyi} and $\lambda_{\mu yi}$ tuning parameters. The peak friction is set by μ_{y_0}.

The pneumatic trail can be estimated with the *Magic tire formula*:

$$t_{pfi} = D_{tf} \cdot cos\left(C_{tf} \cdot atan(B_{tf}\alpha_{fi}) - E_{tf}(B_{tf}\alpha_{fi} - atan(B_{tf}\alpha_{tf}))\right) \tag{2.22}$$

The parameters B_{tf}, C_{tf}, D_{tf} and E_{tf} are tire parameters. Where E_{tf} defines the peak curvature [8][5].

2.4.1.2.3 Tire relaxation is modeling the tire inertia, leading to changes of forces in the tire not happening instantly. This can be included in a reference model with the following equation:

$$\dot{F}_{yi} = A_y \cdot (F_{yi,t} - F_{yi,t-1}) \tag{2.23}$$

Where:

$$A_y = \frac{|v_x|}{L_r} \tag{2.24}$$

Where L_r is referred to as *tire relaxation length* and often is a fraction, approximate $25\% - 50\%$ of the tire circumference [7].

2.4.2 Suspension

Suspension models that include the control arm make the transient movements better represented due to the suspension effect like anti-dive/squat is modeled. The revolute joints for roll and dive degrees are added as a screw joint [7]. From the FBD of a model with linkage, seen

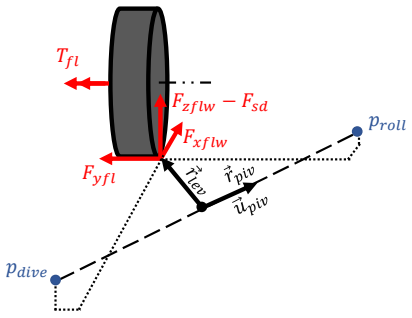

Figure 2.10: FBD of the front wheel suspension.

in Figure 2.10, can the following equations be put up:

$$M_{piv} = \frac{-lead}{2 \cdot \pi} \cdot [F_{xflw}, F_{yflw}, F_{zflw} - F_{sd}] \cdot \vec{u}_{piv} \tag{2.25}$$

$$M_{piv} = (\vec{r}_{lev} \times [F_{xflw}, F_{yflw}, F_{zflw} - F_{sd}] + T_{flw} \cdot [-sin(\delta), cos(\delta), 0]) \times \vec{u}_{piv} \tag{2.26}$$

Where *lead* is how much pitch there is in the screw joint. And the vectors are defined as:

$$\vec{r}_{lev} = [r_{l,x}, r_{l,y}, r_{l,z}] \tag{2.27}$$

$$\vec{u}_{piv} = \left(\frac{1}{|\vec{r}_{piv}|} \right) \tag{2.28}$$

Based on these equations the normal force between the wheel and road can be solved if the force in the dampers and springs are known [7].

2.4.2.1 Normal forces

The normal force needed in the tire lateral force estimation can be calculated with Newton's second law in the yz-plane:

$$F_{zfi} = m \cdot \left(\frac{g \cdot l_i}{2 \cdot L} \pm a_x \cdot \frac{h}{2 \cdot L} \pm a_y \cdot \left(\frac{h_{cgi} \cdot l_i}{L \cdot w} + \frac{\Delta h \cdot c_{i,roll}}{c_{veh,roll}} \right) \right) \tag{2.29}$$

Where h is the height from the ground to the center of gravity, h_{cgi} roll center height in axle, Δh is the height from the roll axle to the center of gravity, $c_{i,roll}$ is the axle roll stiffness, $c_{veh,roll}$ is the total roll stiffness, w is the track width, m and g is the mass and gravitational constant [7]. The normal force can also be estimated by having height sensors on the wheel, then the force in the damper and spring can be calculated with the following equation:

$$F_d = d \cdot c_d \cdot \dot{z} \tag{2.30}$$

$$F_s = k \cdot c_s \cdot (z - z_0) \tag{2.31}$$

Where z_0 is the uncompressed length of the spring and c_s and c_d is the movement ratio between the wheel and spring/damper [7]. Then the normal force between the road and wheel can be solved with the suspension equilibrium in equation 2.25-2.28.

2.4.3 Steering

The steering model calculates the pinion torque from the lateral force and the resulting wheel angles are from a known pinion angle. A FBD of the steering can be seen in Figure 2.11.

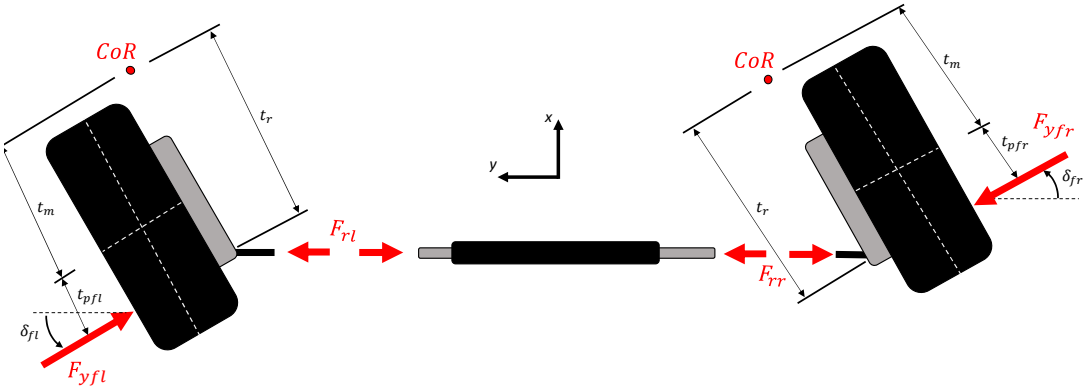

Figure 2.11: FBD of the wheel assembly and the rack.

From the Figure 2.11 can the following three relation be set up:

$$\begin{aligned} I_z \cdot \ddot{\delta}_{fr} &= F_{rr}(t) \cdot cos(\delta_{fr}) \cdot t_r - (t_{pfr}(t) + t_m) F_{yfr}(t) \\ \leftrightarrow F_{rr}(t) &= \frac{I_z \cdot \ddot{\delta}_{fr} + (t_{pfr}(t) + t_m) F_{yfr}(t)}{cos(\delta_{fr}) \cdot t_r} \end{aligned} \tag{2.32}$$

$$\begin{aligned} I_z \cdot \ddot{\delta}_{fl} &= -F_{rl}(t) \cdot cos(\delta_{fr}) \cdot t_r + (t_{pfl}(t) + t_m) F_{yfl}(t) \\ \leftrightarrow F_{rl}(t) &= \frac{-I_z \cdot \ddot{\delta}_{fl} + (t_{pfl}(t) + t_m) F_{yfr}(t)}{cos(\delta_{fl}) \cdot t_r} \end{aligned} \tag{2.33}$$

$$\begin{aligned} \ddot{y}_{ra} \cdot m_{ra} &= F_{rr} - F_{rl} \\ \leftrightarrow \ddot{y}_{ra} \cdot m_{ra} \cdot t_r - I_z \cdot \left(\frac{\ddot{\delta}_{fl}}{cos(\delta_{fl})} + \frac{\ddot{\delta}_{fr}}{cos(\delta_{fr})} \right) &= \\ \frac{F_{yfr}(t) \cdot (t_m + t_{tpfr})}{cos(\delta_{fr})} + \frac{F_{yfl}(t) \cdot (t_m + t_{tpfl})}{cos(\delta_{fl})} & \end{aligned} \tag{2.34}$$

Where $t_{pfi}(t)$ is the tire pneumatic trail and t_m is the mechanical trail and t_r is the distance from the kingpin and the rack [5]. Furthermore, I_z is the inertia for the tire and hub assembly, estimated with the Steiner theorem and assuming that the hub and wheel assembly is in the shape of a solid circular cylinder and the scrub radius is zero:

$$I_z = \bar{I}_z + m_{wa} \cdot (t_m \cdot cos(\gamma_c))^2 \tag{2.35}$$

Where γ_c is the caster angle, m_{wa} is the mass of the wheel assembly and $\bar{I}_z$ is the vertical inertia through the center of mass for the cylinder, which is defined by, where w_{wa} and r_{wa} is the width and radius of the wheel assembly [13]:

$$\bar{I}_z = \frac{1}{4} m_{wa} \cdot r_{wa}^2 + \frac{1}{12} \cdot m_{wa} \cdot w_{wa}^2 \tag{2.36}$$

The wheel angle is calculated from the pinion angle and steering ratio. Ackermann is included, where full Ackermann has the following relation

$$\frac{1}{tan(\delta_o)} = \frac{1}{tan(\delta_i)} + \frac{w_f}{L} \tag{2.37}$$

Where δ_o is the outer wheel angle and δ_i is the inner angle [7].

2.4.4 Friction estimation

There are functions that require a road friction estimation. Common ways are to either use wheel dynamics or complete vehicle dynamics for estimation. The drawback of the wheel approach is its sensibility to high-frequency disturbance. Complete vehicle dynamics require GPS or inertial sensors. Aligning moment can be used for estimation and requires no extra sensors [11][14].

Using longitudinal or lateral dynamics for estimation requires that the force is larger than 60% of the force limit to give an accurate friction coefficient. Because of that, there is a chance that the vehicle stability is put at risk [15][16].

The method of aligning torque requires 30% of the peak friction to be estimated, with an uncertainty of 10%. Because the self-aligning torque has a friction-dependent peak that occurs at a lower slip, compared to the lateral and longitudinal slip, see Figure 2.12 for example [11].

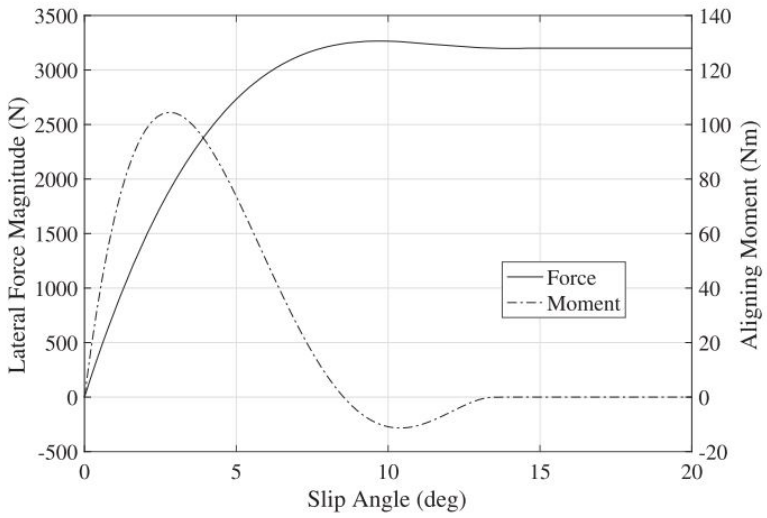

Figure 2.12: Self-aligning drop compared to longitudinal force from [11].

The aligning moment is dependent on the pneumatic trail, which is dependent on the friction coefficient between the tire and the road as seen in the equation below.

$$\mu_i = \frac{t_{fi0} \cdot C \cdot |tan(\alpha_i)|}{F_{zfinom} \cdot 3 \cdot (t_{fi0} - t_{fi})} \tag{2.38}$$

Where t_{fi0} is the initial pneumatic length and C is the cornering stiffness of the tire [17]. In equation 2.38 the trail estimation from *Magic tire formula* can not be used because the model assumes a known friction coefficient. Instead, the trail must be decided with equation 2.32 and 2.33. The lateral force can be estimated based on the slip and the steering torque can either be measured with force-measuring tie-rods or estimated from the EPAS motor sensors.

3
Methodology

A schematic picture of the methodology used for the project can be seen in Figure 3.1. The blocks are described in the following sections. The method is set based on available resources and looking at similar conducted projects.

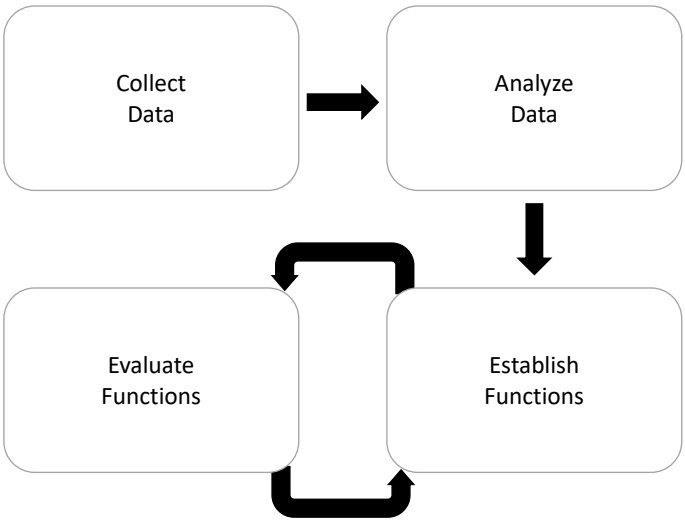

Figure 3.1: Methodology for the project.

3.1 Collect data

The input and output for the steering system during specific conditions and everyday driving were logged. Everyday driving covered both rural and city driving. Two cars were used, one was a Polestar 2 Performance from 2022, the car in which the SbW system should first be implemented. The other car was a HPAS Volvo S60 Polestar Performance from 2016, used as a reference for the steering feedback.

3.1.1 Driving scenarios

For each of the specific conditions, several different driving scenarios were used. Where the course and velocity were varied to create different amplitudes of forces. The different scenarios are specified in the coming sections, for more information see Appendix A:

3.1.1.1 Driving over crest while turning

The purpose of these scenarios was to catch the characteristic of when the feedback torque is decreased in the steering wheel due to front wheel unloading. Therefore the scenarios were driven at the track where there is a combined crest and turn.

3.1.1.2 Driving on a dashed road marking

These scenarios were set up to log the forces in a steering system when the car is driving on dashed road markings. The scenarios had different types of markings.

3.1.1.3 Driving on rutted roads

The scenario here was crossing rutted parts to record the forces going into the steering system. The turning angle over them was varied.

3.1.1.4 Driving with front or rear axle saturated

The last set of scenarios was driving where the front or rear axle became saturated. The gravel track was not used, due to the risk of ruining the external sensors.

3.1.1.5 Logging during scenarios

When driving variables that were used to implement the functions was logged from the cars. These can be seen in Table 3.1.

Table 3.1: Measured signals.

Source	Measu. vari.	Vari. short
CAN	Vehicle velocity	V_x
	Steering angle	θ_p
	Yaw rate	ω_z
	Lateral acc.	a_y
	Motor torque	M_f
External sensors	Rack force	F_r
	Wheel angle	θ_{sw}
	Wheel torque	T_{sw}
	Height Sensor	HS_{ii}

The external sensors are described in the coming sections

Height sensors
The two external height sensors were mounted on the left side's control arms, the stock Polestar 2 has only sensors on the right side. The sensors were the same type and mounted in the same way as on the right sides. Calibration of the sensors was

made by lifting the car with a lift and also loading the car to max weight while measuring the sensor values at different heights.

Torque measuring tie-rods
The tie rods measured the input to the steering system. The sensor was stock tie rods that then have been equipped with strain gauges so that they measure forces. Calibrations were made before mounting them in an external rig.

Torque steering wheel
An additional steering wheel was mounted on top of the stock steering wheel to measure the feedback for the driver. The wheel measured both angle and torque. The steering sensors were calibrated when mounted.

3.2 Analyze data

The next step was to analyze the data. For the Polestar 2 was the aim to understand what the sensors are reading during the specific conditions. For the Volvo s60 was the torque and angle readings analyzed to understand what the output of the function should be for the different situations.

3.3 Establish functions

After that the functions were created in a Simulink model. They calculate the torque sent to the feedback motor, see *Torque Calculation Functions*- block in Figure 2.5. There were five different functions with two supportive blocks, seen in Figure 3.2.

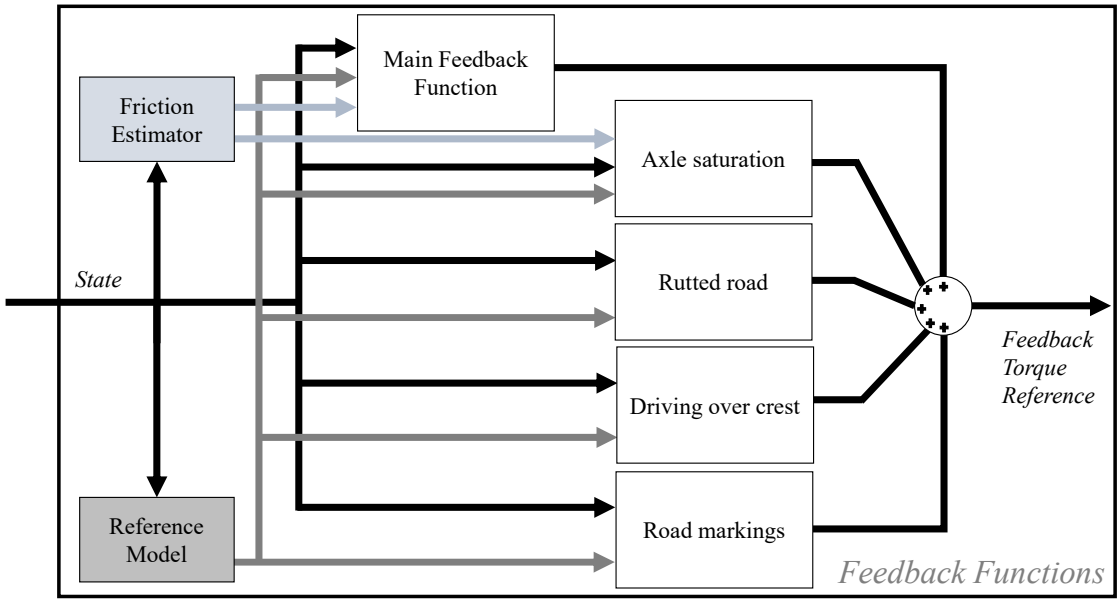

Figure 3.2: Overview of function calculating torque feedback.

Main Feedback Function block continuously decides the basic feedback torque that then the additional functions add to, where the total sum creates the desired feedback. The *Main Feedback Function* block was built up by already established ideas, presented in section 2.3.1. The four additional functions' outputs are zero when the vehicle is not in the specific conditions.

The first additional function detects axle saturation and creates a compensation torque to help the driver stop the saturation. The *Road markings function* detects when a wheel is riding on dashed road markings and creates pulse feedback. The third one is active when the normal force is changed on the front axle, to make the steering either heavier or lighter. While the *Rutted road function* is looking for when the car is crossing the rutted road.

All the functions were set up to take inputs from the Polestar 2 sensors. When a particular situation is found the output is set to mimic a connected system in the same situation.

3.4 Evaluate functions

The evaluation of the function was made by inputting the logged data from the Polestar 2, both from the specific condition and also from everyday driving parts, while comparing their output with the recorded output from the Volvo s60.

The *Establish functions* and *Evaluate functions* were looped over until no further improvement could be established or max number of iteration was reached.

4
Results

The result is a Simulink model consisting of the seven blocks, seen in Figure 3.2. They are described in the coming sections.

4.1 Reference model

The reference model accuracy is set by the demands of the functions. A schematic overview of the model can be seen in Figure 4.1. The grey dotted boxes and the separate blocks are described below.

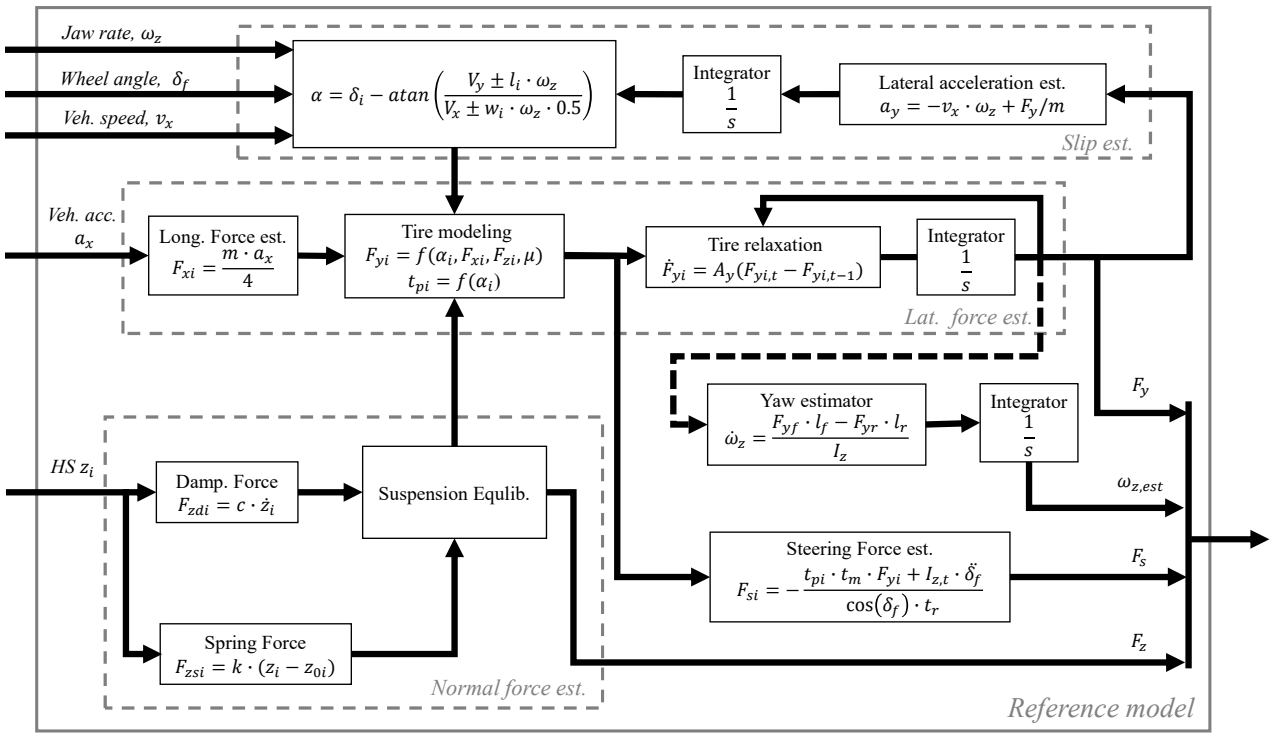

Figure 4.1: Overview of the reference model.

4.1.1 Slip estimation

The slip going into the lateral force is estimated with equations 2.14, using lateral velocity coming from equation 2.12.

4.1.2 Lateral force estimation

This part of the reference model's purpose is to estimate the lateral forces between the tire and the road. This is done by modeling the tire dynamics.

4.1.2.1 Tire modeling

The tires' lateral forces and the pneumatic trail are estimated with the *Magic tire formula*. The longitudinal forces are estimated with Newton's second law assuming that each wheel contributes to the same extent. The parameters for the *Magic tire formula* are coming from estimations based on measurements and data from a similar tire.

4.1.2.2 Tire relaxation

Tire forces are implemented through tire relaxation equations 2.23-2.24, to get a better estimation of tire behavior and to eliminate algebraic loops.

4.1.3 Normal force estimation

The normal force in the tires is estimated using the height sensors, equations 2.30-2.31, and the suspension model, presented in subsection 2.4.2. The linkages are set up by taking the measured roll and pitch axis, from a kinematic and compliance analysis.

4.1.4 Steering force estimation

To transfer the forces estimated in the tires to the rack was the trail, both mechanical and pneumatic, and the location of the steering rack used in equation 2.32-2.34.

The steering transfer function from the pinion angle to the wheels includes the variable ratio, due to the change of angle of tie rod angle, and also the Ackermann, taken from kinematic and compliance measurements. The longitudinal acceleration effect on the steering rack and side forces from cambering effects is neglected.

4.1.5 Yaw estimation

The *Axle saturation function* uses estimated yaw, based on the equation 2.12. The lateral force estimator used has a higher peak force than what the real tire has, to get what the yaw would be if the tire is not sliding.

4.1.6 Performance

The performance of the *Reference model* was evaluated by comparing the estimated steering rack force with the measured rack force from the tie rod to see if they show the same tendency and size. In Figure 4.2 can a comparison on the *Country Track* be seen.

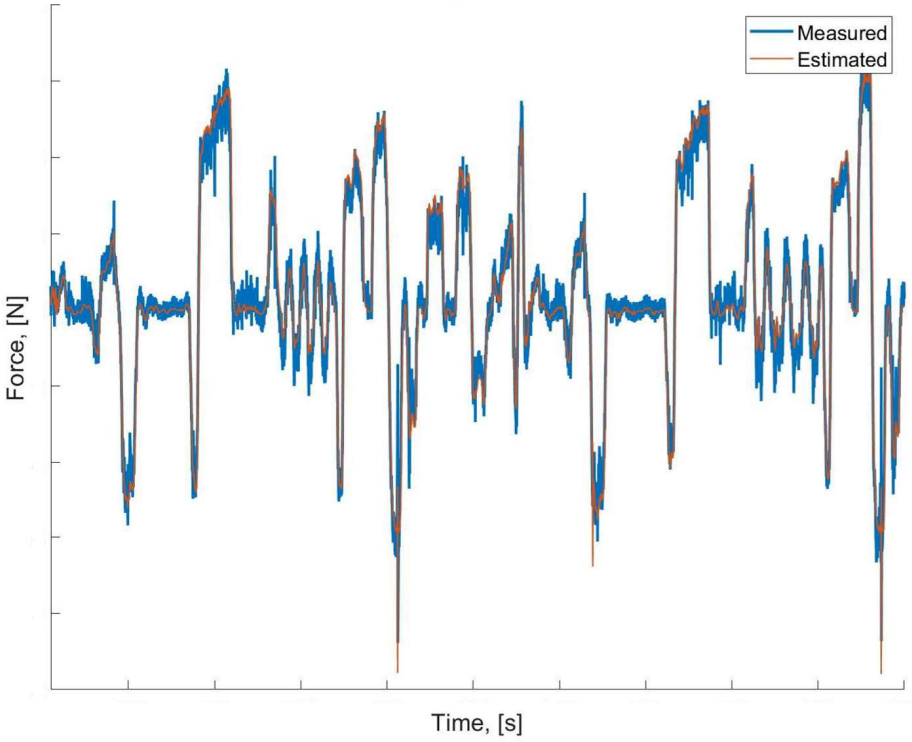

Figure 4.2: Reference model rack and measured rack force on *Country Track*, (CT in Figure A.1).

The performance was also evaluated by looking at the performance of the functions that uses estimated values from the reference model.

4.2 Main feedback function

The resulting *Main feedback function* is built up as presented in section 2.3.1. The virtual steering rack model is based on the *TMSimple* instead of *Magic tire formula*, to decrease the parameters used in the block. The parameters included in the *Main feedback function* are guessed because the exact value depends on the hardware it is implemented in.

4.2.1 Compared with the HPAS

Comparing the measured HPAS steering wheel torque with the reference torque, $M_{tp,ref}$, can be seen in Figure 2.7.

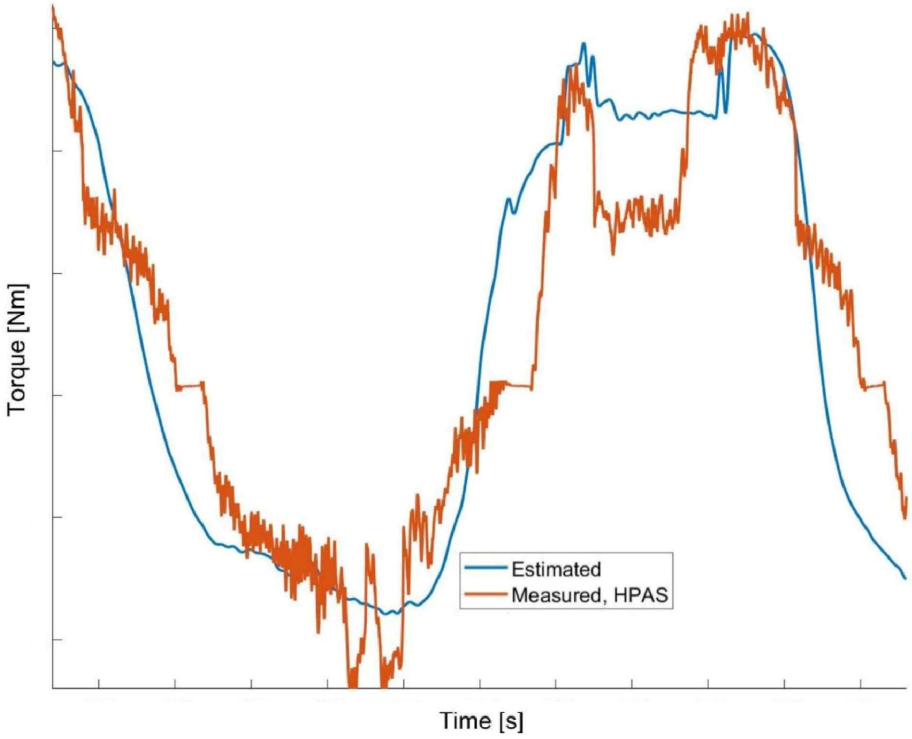

Figure 4.3: Steering wheel torque when driving through the tighter turns at *Handling Track 2*, (HT2 in Figure A.1).

There should be difference between the graphs in Figure 4.3 because the estimation and the measurement are from two different cars. The cars have also not gone the exact same path. The estimation only includes torque from the reference model while the road disturbance contribution is set to zero. The measurements from the HPAS is also showing a dead band when chaining direction. This is probably because the HPAS is having a more pronounced center, compared to the EPAS, which leads to the driver driving more straight between the turns.

But despite the difference in condition for the estimated and measured in Figure 4.3 are there indications of a valid transfer function; The general shape is the same and the decrease due to changes in normal force is similar, more on this in the section for *Turning while driving over crest function.*

4.3 Additional functions

The four functions looking for specific scenarios to output specific feedback to the driver are here presented.

4.3.1 Dashed road marking function

The purpose of this function is to give feedback to the driver when the car is driven on dashed road markings.

4.3.1.1 Main principle

Both of the front wheels' height sensor's readings from the past second are analyzed by looking at the location of the peaks in the compression side of the wheel movement. Peaks that are coming from when a wheel runs over a leading marking edge have a certain range of prominence, width, and value. Peaks that fulfill these demands are stored as the potential start of road markings. The time spacing between them is then compared to see if they have a consistent frequency. The frequency is also compared with the vehicle velocity and allowed length of road marking to see if they are in the right frequency range to be from line marking.

Peaks that have the right frequency and shape, are compared between the front wheels. Peaks that happen close in time between the wheels are assumed to not be from road markings. If there are peaks that fulfill all the demands, then the same analysis is made on the rear tires. Found peaks on the rear wheels, which have the right shape, frequency and are not present on both rear wheels, are compared to the ones found in the front. By calculating the phase shift based on the vehicle velocity, it can be seen if peaks in the front wheel, which in the current time window should have passed the rear wheel, are present. If not they are assumed to be from something else than road marking.

Peaks that full filling all the demands above, are assumed to come from the car riding on road markings. An example of measurement from a wheel can be seen in Figure 4.4.

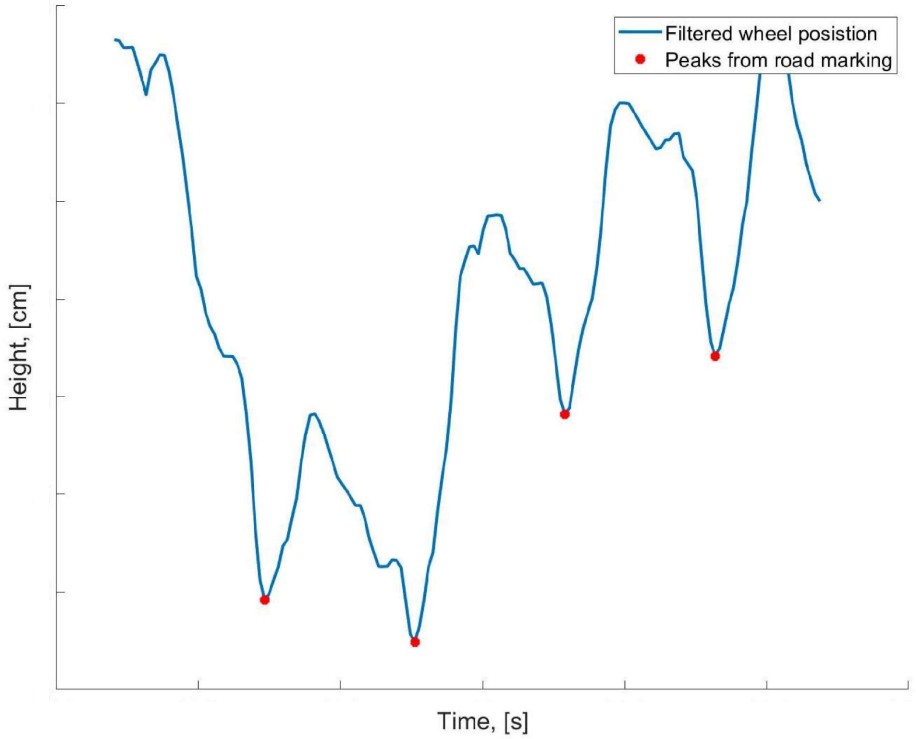

Figure 4.4: Height sensor's reading from the wheel, the leading edge of road markings are marked with a red dot. Height is defined here as the distance from the wheel center to the top of the wheel arch.

If the function detects riding on the road, the output is set to be triggered at the same time as the peaks. The size and length of the torque pulses are set to mimic the pulses measured in the HPAS car, which are dependent on the speed.

The function has parameters that can be tuned to change how sensible it is. The philosophy for the tuning was that it should not be falsely positive, to not annoy the driver.

4.3.1.2 Performance

The performance for this function was decided by letting it analyze the data from the maneuvers where the Polestar 2 was driven on dashed lines, where the lines were highlighted by the driver. The result from the analysis is compared with the highlighting. The function is also verified on the rest of the recorded data to see that it does not react on other parts of the driving. The data consists of five hours of driving where around half an hour is on dashed lines. Where the dashed lines are those on the road between the Töllsjö-Storskogen and Storskogen-Hedared as well as the ones on the high-speed oval and Handling Track 2, see Appendix A for more information. The speed on the lines where varied between 60-110km/h.

The result on the logged data is 99.9% correct when not driving on road markings and 70% correct when driving on road markings. This result is judged to be enough to show that it works.

If the function is allowed to be more false positive it can be tuned to be better at detecting road markings. On the same data as before can the following result be obtained: 95% correct when not driving on road markings and 90% correct when driving on road markings.

The result is also that the height of the line has to be at a certain level to give an indication of the sensors. No exact level has been set but all outer lane lines have worked while some center line has not given any sensors change. In those cases, the logged data has been removed from the overall performance calculation.

4.3.2 Rutted roads function

The purpose of this function is to give feedback to create the same feeling in the steering wheel when crossing a rutted road as in a connected steering wheel.

4.3.2.1 Main principle

There are several versions of this function. None of them are full filling the aim but the result from them is presented below.

In an HPAS car when driving over the rut, there is a steering feedback change. But the main problem is that the input in the sensors when driving over ruts is similar to other cases, where the driver doesn't want feedback from the road in a SbW. This combined with the fact that only one of the front wheels will pass the rut at the time, so there is only one wheel's sensor to rely on, made it not possible to detect only rutted roads.

If both of the wheels are allowed to pass the rut, they can be compared and then detect the rut without being falsely positive. The problem is that if both the front wheel has passed the rut before triggering an output, it is delayed. Because the driver wants feedback in the steering wheel when the front wheel drives over the rut.

4.3.3 Axle saturation function

The function's purpose is to help the driver to stop the car from having an axle saturated. This is not implemented to mimic the mechanical system but as an improvement of the steering feedback.

4.3.3.1 Main principle

This function uses the same principle as some of the electronic stability control systems. But instead having the steering wheel torque as output.

The function calculates, based on the velocity and the steering angle, the optimal yaw rate, which is when no axle is saturated. It uses equation 2.12. The lateral forces are estimated with the same tire model as the real one but with a higher peak force. This makes it calculate the yaw when no axle is saturated. Then if the measured yaw rate is larger than the optimal yaw, the rear axle is saturated and if the measurement is less then the front is saturated.

The function requires that the reference model is able to handle on-limit handling and transient driving, which is often the case with saturated axles. Therefore was the suspension equilibrium added.

When the function detects rear saturation, it adds a counteracting steering torque that is proportional to the current force to help stop the slide.

An example of the optimal and measured yaw rate can be seen in Figure 4.5, where the rear axle is saturated short after times instances A, B and C.

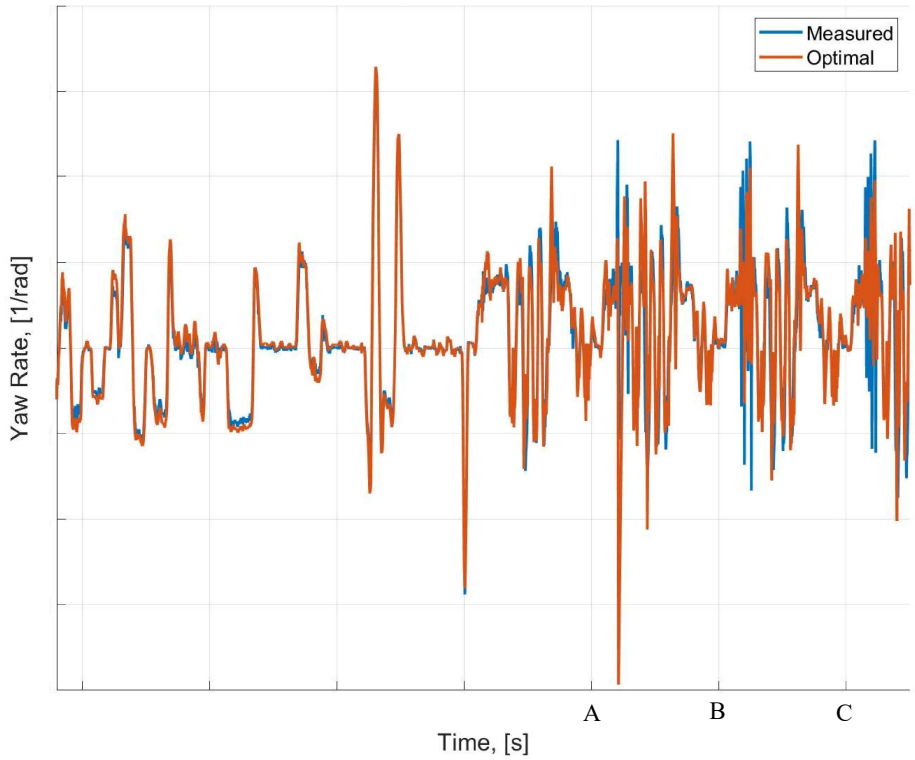

Figure 4.5: Axle saturation when driving on the *Handling Track 2*, (HT2 in Figure A.1).

4.3.3.2 Performance

The performance for this function was set in the same way as for driving on dashed lines, by letting it analyze the data from the maneuvers where the Polestar 2 was driven with an axle saturated. During those measurements is the saturation parts highlighted by the co-driver. The result from the analysis was compared with the highlighting from the measurement to see if the function found all saturation while not being falsely positive. The function is also verified on the rest of the recorded data to see that it does not react on other parts of the driving. On the data, it detects all places where an axle is saturated while not reacting to other parts. The logged data consist of axle saturation on four different tracks with two different drivers. The speed while saturation varies between 80-100km/h.

4.3.4 Turning while driving over crest function

This function's purpose was to detect the unloading of the front tires and outputs a torque that makes steering lighter, mimicking the HPAS.

4.3.4.1 Main principle

Unloading the front will give lighter steering through the *Main feedback function* because the reference model uses a normal force estimator based on the height sensors. An external equation has also been created which does detect these situations.

The function has a running height sensors mean and when the current height goes away from the mean is the car assumed to be loaded or unloaded. The output for the scenarios is a torque which makes the steering lighter for unloading and heavier for loaded.

4.3.4.2 Performance

The function full fills the aim with a torque change, due to the normal force of the tires. An example of a torque change over a crest can be seen in Figure 4.6, where the estimated steering feedback torque from the *Main feedback function* is compared with the torque measured from the HPAS car when driving over the same crest with a constant turning radius.

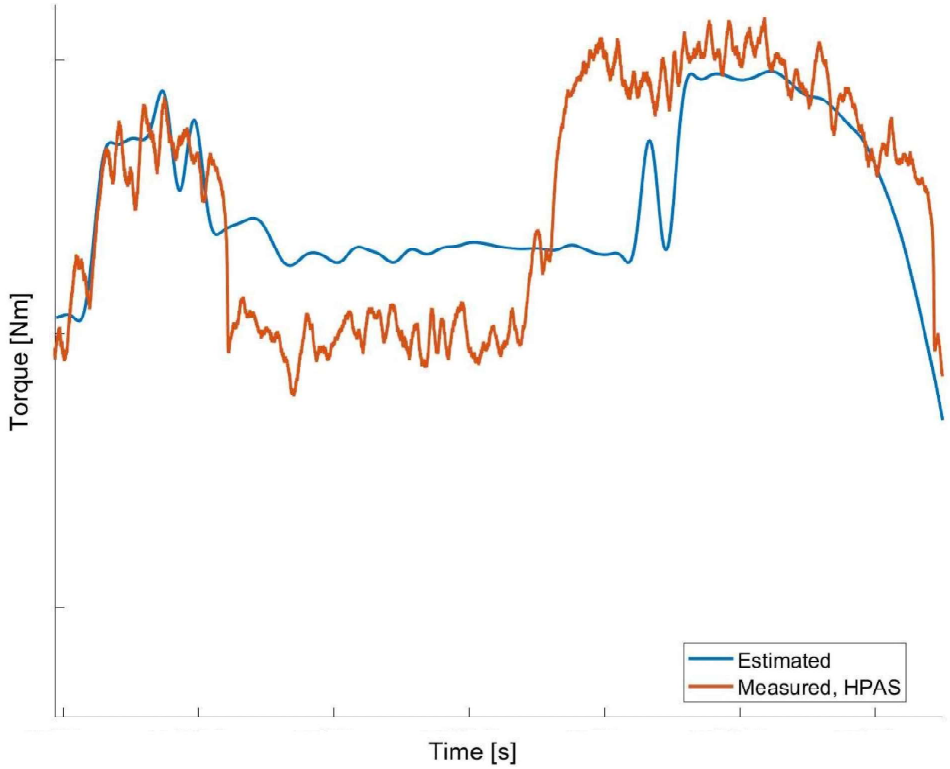

Figure 4.6: Steering wheel torque when driving over a crests at *Handling Track 2*, (HT2 in Figure A.1).

As described in section 4.2.1 is the comparison in Figure 4.6 not optimal. But despite that can it be seen that both curves show a unloading when driving over the crest. The amount of unloading for the estimation can be increased with a tuning parameter to mimic the HPAS unloading better. Now the amount of unloading is instead set to be as realistic as possible, based on the tire and car parameters for the Polestar 2. That is done because the aim is to mimic how the Polestar 2 would feel if it was a mechanical connected steering system and not the Volvo s60.

The difference in how long time where the tire is unloaded could be from the variation in speed and driving angle over the crest, the aim was to have these equal but there are not the exact same. The car's weight and suspension inequality is probably also a contributing factor.

4.3.5 Friction estimation function

The reference model, shown in Figure 3.2, estimates force based on a friction coefficient. Where a lower coefficient leads to decreased feedback to the driver indicating less available grip. The Polestar 2 has a friction estimation implemented. But the result is not available on the CAN-bus system which means that this work has been unable to use it.

Even though there is a working estimator that potentially can be used in the future

SbW is a friction estimator created. The limitation is that it's only developed on asphalt.

4.3.5.1 Main principle

Two different versions are tested. The first estimates the friction by dividing the lateral and longitudinal force by the normal force. Because the lateral force from *Magic tire formula* is based on an assumed known peak friction, they could not be used. Instead are the forces measured from the tie rod used, transformed by using the estimated pneumatic trail and the known front suspension geometry.

The drawback is that the coefficient can only be estimated when driving close to the limit and that tie rod forces measurement are used. The tie rod force measurement could be replaced with the steering force estimation from the EPAS motor. But it could lead to less accurate readings.

The second version is a friction estimator based on aligning torque, as described in section 2.4.4. The pneumatic trail is estimated using the force-measuring tie rods. It can be done with the estimated torque on the EPAS motor but to minimize the sources of errors the tie rods are used here.

4.3.5.2 Performance

The forces-based version gave an expected result, the friction estimation is too low with lower forces but going closer to on-limit handling gives a better result. it can not be verified because the exact friction coefficient is not known. An example of the performance of this function on *Handling Track 2* on a dry day can be seen in Figure 4.7.

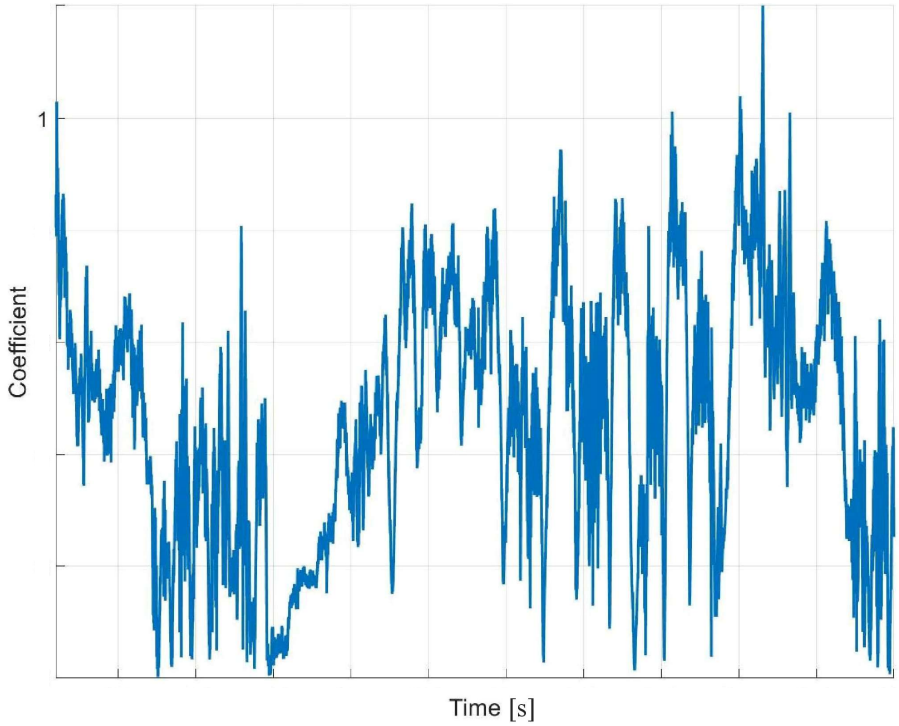

Figure 4.7: Friction Coefficient Estimation lateral, on *Handling Track 2*, (HT2 in Figure A.1).

The aligning torque gave expected values when driving close to steady state. For transient driving, the function is giving unreasonable results. Driving without any larger side acceleration is also unreasonable, but that was expected. An example of the performance of this function on the same data as Figure 4.7 can be seen in Figure 4.8, where the y-axis is zoomed in to show the range where the result was expected to be.

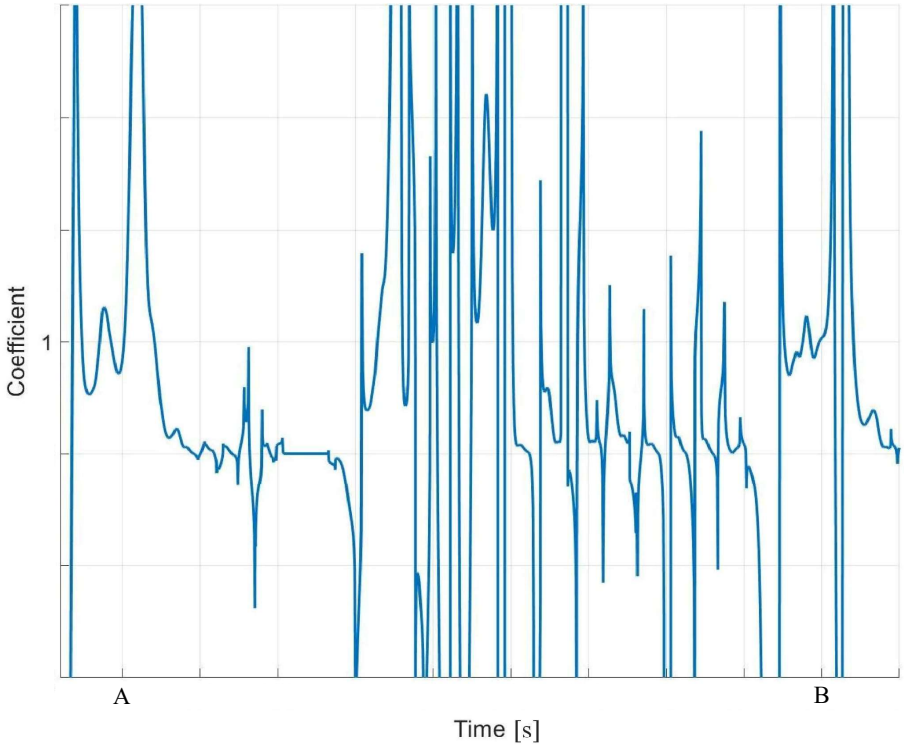

Figure 4.8: Friction Coefficient Estimation aligning torque, on *Handling Track 2*, (HT2 in Figure A.1).

In the parts where the reading is close to reasonable, around time instances A and B, the car is doing turns close to steady states.

5
Discussion

This chapter discusses the main parts of the model. The purpose of the model is to test different approaches that could be implemented in future SbW. Because of that has no function been evaluated in a SbW car. This could be a source of error because even if the functions work on logged data the case could be that it doesn't work as it should in a SbW car.

5.1 Reference model

The purpose of the reference model was achieved. It estimates the unknown variables needed for the functions. But it does that with some assumptions and there are also parts which can be improved.

5.2 Assumptions

Because the model outputs steering feedback, which is primarily based on lateral forces, was the decision only to estimate the longitudinal forces by Newton's second law and assume that all wheels contribute equally to the acceleration, which is not the case for the Polestar 2 with open differentials driven on uneven friction.

This assumption affects the steering feedback in two ways, it is indirect through the functions where the longitudinal force is used to calculate the output torque. It also affects directly, by the fact that scrub radius combined with longitudinal forces creates torques going into the steering rack. When the longitudinal forces are not the same they create a resulting force in the rack. A more accurate longitudinal force estimation could be implemented but it would require more computing power and result in a more complex reference model.

5.2.1 Improvements

The parameters for the tire models could be improved because they are estimations or taken from similar tires. Better tire parameters could lead to a more accurate reference model. Including the camber effect, wheel lifts, bump stops and compliance in the suspension could improve the on-limit and transient handling.

5.3 Main feedback function

The *Main Feedback Function* is based on already established ideas. The function requires that the parameters connected to the steering hardware are known. Because no hardware was set to implement the function, these parameters are currently estimations. The only verification possible for the function was by comparing the estimated feedback, based on the Polestar 2 measurement, with the measured from the HPAS vehicle. As mentioned in the section 4.2.1 is the comparison not optimal and include many sources of error. This function must therefore be developed and evaluated further with a valid evaluation method.

5.4 Dashed road marking function

This function gives a promising result. But the function can not find markings that are worn down to the point where they do not give any change in ride height sensors. The conclusion from the logged data is that all of the outer lane lines have worked while some center lines have been too worn down. The line that has been worn has generally been in corners, probably from cars cutting the corner. The marking detection could probably be improved with better height sensors.

Another aspect is the evaluation of the function. Because the function is evaluated by comparing it with the data recorded. Where the driving on lines is highlighted. The decision, when the car is driven on a line, is taken by the persons in the car. It is taken based on the placement of the car as well as the movement and sound of the vehicle. But there could be misjudgment, both false positive and negative. This can therefore affect the performance of the function.

5.4.1 Assumptions

The assumption is that peaks from road markings are in a range of prominence, width, and height. These have worked on the logged data but there could be other road marking that doesn't lay inside this range and therefore are missed.

Another assumption is that a road marking can not add peaks on both wheels on an axle at the same time, the aim was to catch dashed lines parallel to the road. This is added to remove peaks coming from unevenness in the road but could contribute to false negative readings. The last assumption, that the peaks must be present on both the front and rear wheels, is included to remove peaks coming from measurements error and loose objects. This assumption could lead to error when the car is turning extensively resulting in that only the front wheels are riding on road markings.

5.4.2 Other versions

A version of this function investigated using FFT to detect the frequencies in the height. The problem is that because of the low frequencies from the marking, FFT needs to have a window longer than 2 seconds to provide a useful result, thereby delaying the feedback to the driver.

Another way tested was to look at the wheel velocity sensors, the wheels going over the marking have to roll a further way, therefore going faster compared to the other wheels. But this method was ruled out because no noticeable change was seen in the wheel velocity.

5.4.3 Improvements

An improvement could be if it was combined with visual cameras. The function could then be activated only when the camera is detecting that the car is approaching the markings. This could enable a more sensitive tuned function because the time window for it to be false positive is smaller.

It could be argued that this function should be allowed to be more false positive even because it would lead to an increase in sensing road markings, which would lead to increased safety. The feedback from the function could also be made more subtle to decrease the chance of it disturbing the driver. But then the risk is that the driver misses the feedback.

5.5 Rutted road function

This function does not fulfill the aim, the external change effect on the sensor is similar to other scenarios. That makes it impossible to catch the rutted road without letting others not wished disturbances being feedback to the driver. After both front wheels have passed the rutted part, then it can be sensed as a rutted road without other cases being falsely detected. But then the feedback to the driver is sent after the rut and therefore the purpose of the function is missed. Changing the height sensors to more accurate ones could maybe make it possible to detect the rutted part without being falsely positive.

It was tested using a combination of sensors to get a more accurate reading of the rut. But because of the delay between the movement of the wheel and the body, the sensors onboard the body have too long delay. The best result is therefore found by using the same principle as in the road marking function, looking at the sensors close to the wheels. This function was tested using wheel velocity readings. But no unique changes were possible to detect.

5.6 Axle saturation function

This function is not tried out on other surfaces than asphalt and therefore it can not be verified if it works or not on other types of roads. But on the logged data gives it a promising result. The performance is here based on comparing it to logged data where the axle saturation is marked out by the co-driver. This could be a source of error because as described in section 5.4 could there be instances where the saturation is marked false positive or negative.

Because axle saturation can occur when driving transient the function did require that the additional suspension model was added to the reference model. Before it was delayed and missed some of the trends in the forces at transient driving. There is still some room for improvement when sliding in several turns after each other, where some delays can occur, probably connected to errors in transient driving estimation. Adding more detail to the suspension model could maybe help limit these.

Worth pointing out is that the optimal yaw estimation is sensitive to changes in car parameters combined with transient on-limit handling. It could maybe be solved by tuning the estimator or having some type of way of sensing the change of parameters of the car, like inertia, and weight.

5.7 Turning while driving over crest function

This function full fills its aim and can either be implemented directly into the reference model or as a separate function. All changes of the normal force are sensed as changes in feedback to the driver. The subjective best feedback could maybe be created if only slower and larger normal force changes lead to a feedback change.

5.8 Friction estimation function

Because the true friction coefficient was not measured, the result conclusion is based on a guessed correct coefficient. These estimators should be tested on different surfaces to see how they are affected by different friction coefficients.

The friction estimation based on lateral dynamics is only getting close to accurate when close to the limit of the tires, which is expected. The aligning torque gives the inaccurate result and only gives values that could be argued to be close to accurate when steady-state cornering. This is not expected because there are papers with similar friction estimations and variables that show accurate values for the transient situations: step steer and sinus-steer. The errors could be due to the simplified longitudinal force or that this friction estimation can only handle simpler transient driving.

6
Conclusion & Future work

6.1 Conclusion

The conclusion from the thesis is that four of the created functions have shown potential, with the help of the available signals, to detect their aimed scenarios and create a mimicked HPAS feedback output for a SbW. Those are the *Dashed road marking function*, *Axle saturation function*, *Driving over crest function* and the *Main feedback function*. But further work with developing, validating and implementing the functions in a car must be done

The *Rutted road function* is not showing to be possible while the *Friction estimator function* is not working as it should because it is only giving values that could be seen as close to accurate when close friction limit or transient driving.

6.2 Future work

Future work could be to implement the functions in a car. It would first require adapting them to the hardware available in the car and ensuring that they are stable and run in real-time. Then the functions could be improved further by being able to sense if the feedback is reasonable and natural while driving. Connected to that could a potential future work be to combine the functions with a disturbance estimator and controller, seen in Figure 2.5.

It would also be interesting to use the functions in different environments and car parameters configuration. Another part is to investigate the change of performance in the function if the sensors are replaced.

An area for further work is to improve the reference model. This could be done by adding more of the physical phenomena to the model, like longitudinal slip estimation and bushing compliance. Another improvement is to decrease the computer power required by the functions.

Bibliography

[1] Bosch, ed. *Steer-by-Wire*. URL: https://www.bosch-mobility-solutions.com/en/solutions/steering/steer-by-wire/.

[2] D. Gualino and I. Adounkpé. *Force-feedback system design for the steer-by-wire: optimisation and performance evaluation.* IEEE, 2006.

[3] M. Harrer and P. Pfeffer. *Steering Handbook*. 2017.

[4] A. Finne and L. Ström. *Road Feedback in a Steer-by-Wire System for a Passenger Car*. Linköping University, 2022.

[5] T. Chugh. *Steering control for haptic feedback and saftey functions*. Chalmers University, 2021.

[6] M. Johaneesson and H. Lillberg. *Investigation of Steering Feedback Control Strategies for Steer-by-Wire Concept*. Linköping University, 2018.

[7] B. Jacobson. *Compendium in Vehicle Motion Engineering*. Chalmers University, 2022.

[8] H. Pacejka. *Tire and Vehicle Dynamics*. Oxford : Elsevier Science Technology, 2012.

[9] G. Rill and A. A. Castro. *Road Vehicle Dynamics*. 2020.

[10] C. Lex. . *Estimation of the Maximum Coefficient of Friction between Tire and Road based on Vehicle State measurements*. 2015.

[11] C. Ahn, H. Peng, and H. E. Tseng. "Robust estimation of road friction coefficient". In: *Control Systems Technology, IEEE Transactions on, vol. 21, 1-13* (2013).

[12] C. Rex. *Estimation of the Maximum Coefficient of Friction between Tire and Road Based on Vehicle State Measurements*. Graz University of Technology, 2015.

[13] M. M. Japp. *Formulas in mechanics*. Chalmers University, 2010.

[14] S. A. Chang. *Robust Estimation of Road Friction Coefficient for Vehicle Active Saftey System*. The University of Michigan, 2011.

[15] A. Albinsson. "Design of Tyre Force Excitation for Tyre-Road Friction Estimation". In: *Vehicle System Dynamics, 55:2, 208-230* (2016-11-02).

[16] E. Craig. "Rapid Road Friction Estimation using Independent Left/Right Steering Torque Measurments". In: *Vehicle System Dynamics, 58:3, 377-403* (2020).

[17] Y. J. Hsu, Laws S. M., and Gerdes J. C. "Estimation of Tire Slip Angle and Friction Limits Using Steering Torque". In: *IEEE TRANSACTIONS ON CONTROL SYSTEMS TECHNOLOGY, 18:4* (2010).

A

Figures for maneuvers

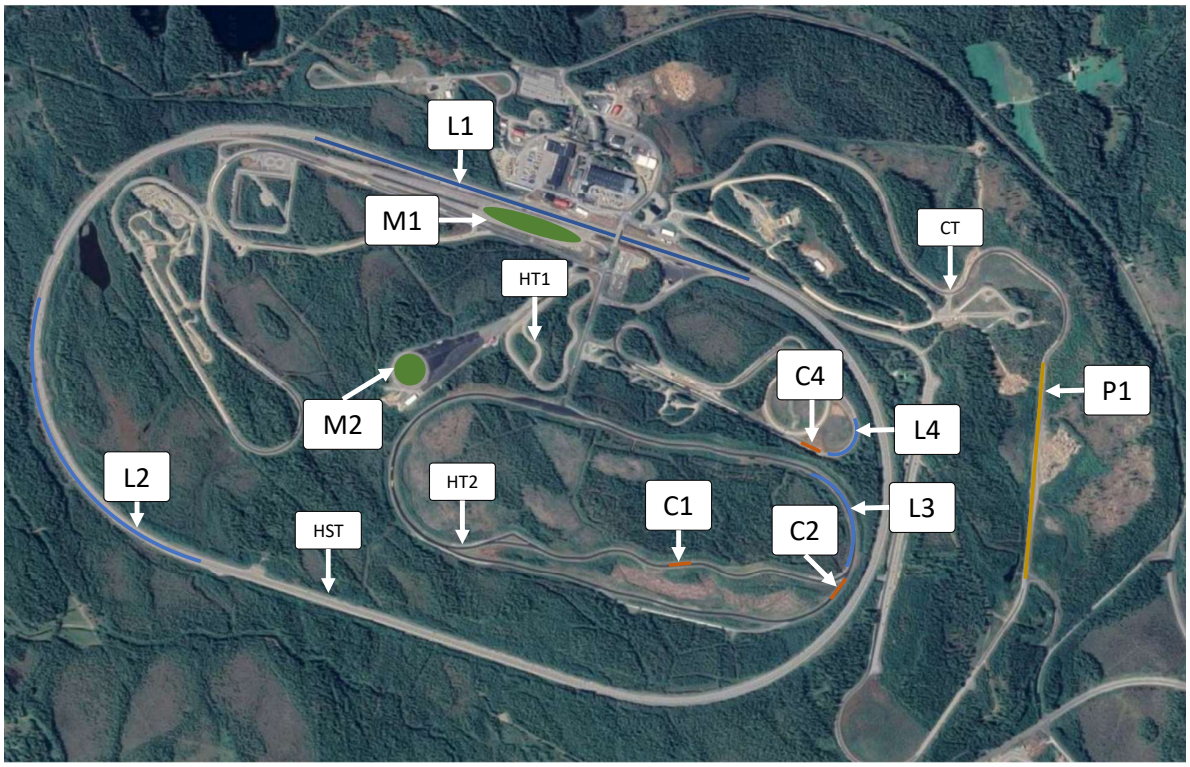

Figure A.1: Hällered Proving Ground with the stages marked out for the different maneuvers, picture taken from Google Maps

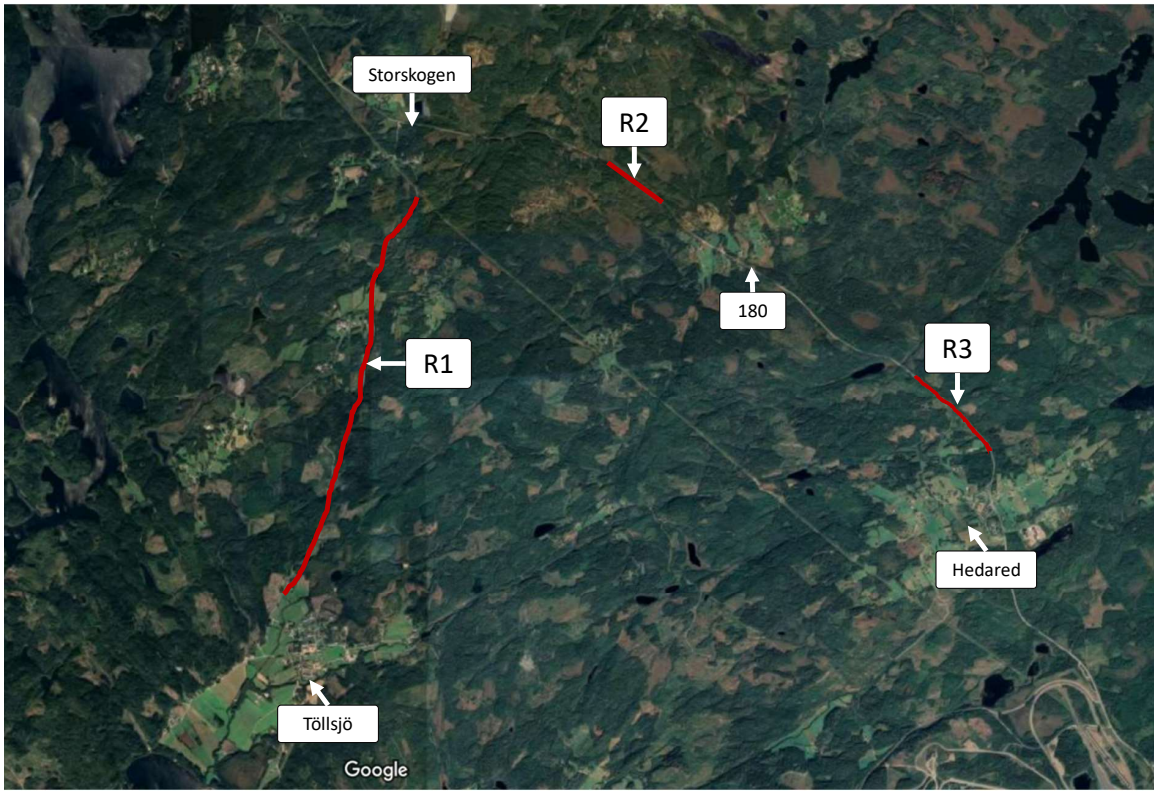

Figure A.2: Stages that are outside of the proving ground, picture taken from Google Maps

The different stages are listed below

- Turning over crest: C1-C4
- Driving on road marking: L1-L4 & R1-R2
- Rutted roads: P1
- Under- and oversteering: M1, M2, HT1 and HT2

DEPARTMENT OF SOME SUBJECT OR TECHNOLOGY
CHALMERS UNIVERSITY OF TECHNOLOGY
Gothenburg, Sweden
www.chalmers.se

CHALMERS
UNIVERSITY OF TECHNOLOGY